Journal of The Electrochemical Society, **157** (6) B914-B919 (2010)
0013-4651/2010/157(6)/B914/6/$28.00 © The Electrochemical Society

Sulfonated Polysulfone/POSS Nanofiber Composite Membranes for PEM Fuel Cells

Jonghyun Choi,[a,*] Kyung Min Lee,[a] Ryszard Wycisk,[a,] Peter N. Pintauro,[b,**,z] and Patrick T. Mather[c]**

[a]*Department of Chemical Engineering, Case Western Reserve University, Cleveland, Ohio 44106, USA*
[b]*Department of Chemical and Biomolecular Engineering, Vanderbilt University, Nashville, Tennessee 37235, USA*
[c]*Syracuse Biomaterials Institute, Biomedical and Chemical Engineering Department, Syracuse University, Syracuse, New York 13244, USA*

A class of nanofiber-based polymer/particle proton exchange membranes (PEMs) is described for use in H_2/air fuel cells that operate at low humidity. The membranes were fabricated from electrospun nanofibers composed of sulfonated poly(arylene ether sulfone) (sPAES) with sulfonated polyhedral oligomeric silsesquioxane (sPOSS) as a proton conductivity enhancer. The void space between nanofibers in an electrospun mat was filled with a mechanically robust and chemically stable UV-cross-linked polyurethane to create a gas impermeable membrane. Membranes with nanofibers composed of 2.1 mmol/g ion-exchange capacity sulfonated polysulfone with 40 wt % sPOSS and a nanofiber volume fraction of 0.70 exhibited a proton conductivity of 0.094 S/cm at 30°C and 80% relative humidity (RH), which was 2.4 times higher than that of Nafion 212 at the same conditions. The high proton conductivity was attributed to the high concentration of protogenic groups in the sPAES/sPOSS nanofibers and the ability of the nanofibers to hold water, where the equilibrium water-vapor uptake of the membrane was 3.8 times higher than that of commercial Nafion at 30°C and 80% RH.
 [DOI: 10.1149/1.3392294]

Manuscript submitted November 23, 2009; revised manuscript received March 17, 2010. Published April 28, 2010.

Historically, most of the research work on Nafion replacements for proton exchange membrane (PEM) fuel cells has proceeded along two lines: (*i*) the development of new polymers with alternative backbone chemistries and various protogenic groups [e.g., sulfonated poly(arylene ethers) and phosphonated or sulfonated polyphosphazenes[1-3]] and (*ii*) polymer doping through an addition of inorganic components (e.g., silica,[4-7] zirconium phosphate,[8-10] or heteropolyacids[11-13]) to enhance water retention, add acidic ion-exchange sites, improve membrane stability at elevated temperatures, and/or induce self-humidification.[14] To ensure high proton conductivity, high ion-exchange capacity (IEC) polymers were utilized, but such polymers swelled excessively in water (with a loss in mechanical properties) and were brittle when dry.[15-17] The addition of inorganic particles to a polymer often exacerbated the brittleness problem. To minimize these deficiencies, various blending or copolymerization strategies were utilized,[18-20] with only moderate success. Although some improvement in the low humidity fuel cell operation was observed with a composite membrane, as compared to an unmodified ionomer film (often DuPont's Nafion), the power outputs were generally low.[21-23]

In the present study, an implementation of the polymer/particle composite strategy is demonstrated, where fuel cell membranes are fabricated by electrospinning nanofibers composed of a proton conducting polymer with proton conducting, water-retaining inorganic nanoparticles. Specifically, a nanofiber mat was electrospun from sulfonated poly(arylene ether sulfone) (sPAES) to which sulfonated polyhedral oligomeric silsesquioxane (sPOSS) nanoparticles were added to improve water retention and proton conductivity. The interfiber voids were filled with an acid- and temperature-resistant hydrophobic photocurable polyurethane. This uncharged polymer surrounds each nanofiber, restricts fiber swelling in water, and provides mechanical strength to the membrane, thus permitting a higher loading of inorganic particles and the use of fibers with a fixed-charge concentration much greater than that which is practical in a homogeneous ion-exchange membrane. The resulting phase-separated nanofiber/matrix-polymer morphology is similar to the desired/ideal bicontinuous structure in a block copolymer system, but there is more flexibility in our fabrication approach. Thus, the ionomer, fiber diameter, fiber volume fraction, and inert polymer can be selected independently. Additionally, the present approach might represent an effective way to fabricate a fluorocarbon-free "green" PEM with good mechanical properties and a conductivity exceeding that of Nafion at RHs less than 100%.

Experimental

Materials.— 4,4′-Dichlorodiphenyl sulfone (DCDPS, Aldrich) and 4,4′-biphenol (BP, Acros Organics) were recrystallized from methanol and acetone, respectively. Fuming sulfuric acid (SO_3 content ~30%, Aldrich) and toluene (Aldrich) were used as received. *N*-Methyl-2-pyrrolidone (NMP) solvent (Acros Organics) was dried over calcium hydride (CaH_2) and distilled under a reduced pressure before use. Potassium carbonate (K_2CO_3, Aldrich) was dried in a vacuum oven at 110°C for 16 h. Sulfonated octaphenyl polyhedral oligomeric silsesquioxane (with the structure shown in Fig. 1) was purchased from the Michigan Molecular Institute (Midland, MI) and used as received.

Polymer synthesis.— First, 3,3′-disulfonated DCDPS (ds-DCDPS) was prepared by the sulfonation reaction of DCDPS with fuming sulfuric acid (mol ratio of fuming sulfuric acid to DCDPS = 3.3:1) at 110°C for 6 h under a nitrogen atmosphere. After neutralization with base, the product was purified by recrystallization from an isopropanol/H_2O mixture (3/1 v/v). Complete disulfonation of DCDPS was confirmed by ^1H NMR spectroscopy (in dimethylsulfoxide-d6, Varian 300 MHz). sPAES copolymers (with the structure shown in Fig. 2) were prepared via nucleophilic aromatic condensation polymerization. To obtain high molecular weight sPAES copolymers, highly purified and completely dried monomers were used. DCDPS (1.034 g, 3.6 mmol), ds-DCDPS (4.124 g, 8.4 mmol), BP (2.2345 g, 12 mmol), and potassium carbonate (1.935 g, ca. 14 mmol) were charged to a three-neck flask equipped with the Dean–Stark trap and a reflux condenser. Dried NMP (10 mL) and toluene (5 mL) were added, and the reaction temperature was increased slowly to 150°C with refluxing for 3 h, at which time the Dean–Stark trap was drained. The temperature was then increased slowly to 190°C and refluxed for 16 h under a nitrogen atmosphere. To further increase the molecular weight of the sPAES copolymer, a small amount of DCDPS monomer (~1 mg) was added several times per hour to the sPAES solution until the

* Electrochemical Society Student Member.
** Electrochemical Society Active Member.
z E-mail: peter.pintauro@vanderbilt.edu

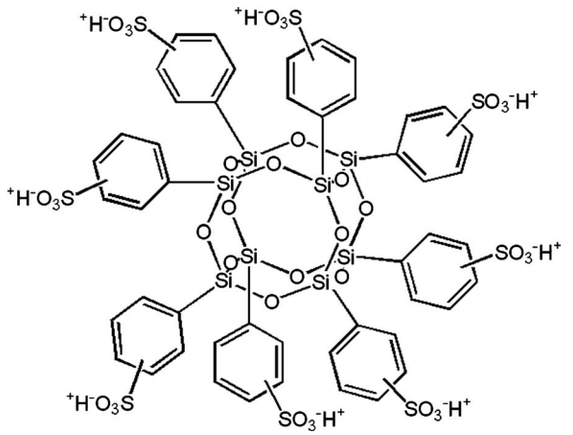

Figure 1. Chemical structure of sPOSS.

reaction solution became very viscous (evidence of a coupling reaction). This final sPAES solution was precipitated into distilled H_2O and the resulting fibrous solid was washed several times with distilled H_2O to remove salts followed by vacuum drying at 120°C for 48 h. The actual ds-DCDPS/DCDPS ratio in the sPAES copolymer was 0.52/0.48, as determined from ^1H NMR spectroscopy (Varian 300 MHz). The number-averaged molecular weight (70,500 g/mol) was determined from gel permeation chromatography (Waters) based on polystyrene standards using a 0.01 M LiBr/DMF solution as the eluent at a flow rate of 1 mL/min. The intrinsic viscosity of the polymer (0.72 dL/g) was measured using a Cannon Ubbelohde viscometer at 25°C (0.05 M LiBr/NMP was used as the solvent to minimize the polyelectrolyte effect). The polymer IEC was determined by a standard titration method. sPAES polymers with a high IEC (2.1 mmol/g) were used to prepare nanofiber network composite membranes. In a similar way, sPAES with a ds-DCDPS/DCDPS ratio of 0.58/0.42 and an IEC of 2.5 mmol/g was also synthesized.

Fabrication of nanofiber network composite membranes.— Nanofiber network composite membranes were fabricated using a four-step process: (*i*) electrospinning a nanofiber mat, (*ii*) mechanical compaction of the mat to increase the volume density of fibers, (*iii*) welding of intersecting fibers, and (*iv*) embedding an inert polymer into the void space between fibers. Neat sPAES nanofibers were electrospun using a 30 wt % sPAES copolymer solution in 2-butoxyethanol (2.1 mmol/g IEC sPAES, with the polymer in the H^+ form). The fiber mat was prepared using a custom-made electrospinning apparatus at a voltage of 10 kV, a polymer solution flow rate of 0.05 mL/h, and a spinneret-to-collector distance of 6 cm. Fibers were collected on a rotating aluminum drum (1000 rpm), which oscillated laterally (horizontally) at a speed of 25 cm/s. A large nanofiber mat was produced (16 × 6 cm) with a uniform fiber volume fraction and mat thickness. To prepare 2.1 mmol/g IEC sPAES fibers with sPOSS, the electrospinning solvent was 2-butoxyethanol and the sPAES/sPOSS weight ratio in the electrospinning solution was 60/40. sPAES/sPOSS nanofibers were collected on the rotating and oscillating drum apparatus under the following conditions: 14 kV applied voltage, 0.05 mL/h polymer solution flow rate, and 6 cm spinneret-to-collector distance.

The fiber volume fraction of the electrospun mats ranged from 0.18 to 0.22 (the fiber volume fraction was determined as the ratio of the mat density to the density of a homogeneous polymer film). After drying at 60°C for 16 h, the mats were mechanically compacted for 3 min at room temperature using a bench-top hydraulic press (Carver, Inc., model 3912). A pressure of 10,000 psi increased the fiber fraction from 0.20 to 0.60. Nanofibers in a densified mat were welded at fiber intersection points by exposing the mat to 2-butoxyethanol vapor in a sealed chamber at 25°C for 30 min. After welding, the fiber volume fraction in a mat increased from 0.60 to 0.70–0.75.

Densified and welded mats were impregnated with UV-curable Norland Optical Adhesive (NOA) 63. The mats were immersed in the liquid form of NOA 63 under vacuum at 45°C for 1 h. Excess NOA 63 was removed from the mat surfaces, followed by UV light curing (365 nm wavelength) for 2 h (1 h per each side of the mat). The quality and morphological features (nanofiber diameter and fiber diameter distribution) of the initial nanofiber mat, the densified mat, and the densified and welded mat were determined using high resolution scanning electron microscopy (Hitachi field-emission-scanning electron microscope S-4500).

Membrane characterization.— Membranes were characterized in terms of proton conductivity at 30 and 80°C, where the RH was varied from 30–95%, and equilibrium water uptake (at 30°C with 10% < RH < 90%). Before proton conductivity measurement, membranes with neat sPAES nanofibers were pretreated in 1 M H_2SO_4 at room temperature for 16 h and then washed several times with deionized water (over a period of 6 h) to remove excess acid. To ensure complete retention of high IEC sPOSS particles, nanofiber network composite membranes containing sPOSS were not treated with acid or water. The proton conductivity of water-vapor equilibrated membranes was measured in the lateral (in-plane) direction by an ac impedance technique using a BekkTech LLC, four-electrode cell (model BT-110) mounted inside a programmable temperature/humidity chamber (Espec model SH-241). Membrane water uptake tests were performed using a dynamic water-vapor sorption analyzer (model Q5000SA, TA Instruments). Each sample was predried at 80°C and 0% RH for a maximum of 200 min until the sample weight stabilized (which occurred when the weight change over a 5 min time interval was less than 0.001%). The testing temperature was set and the humidity was increased slowly from 10–90% RH at a stepsize of 10%. Sample equilibration at a given humidity required no more than 100 min (where the weight stabilization criteria was 0.001% in 5 min).

Results and Discussion

The general concept of a nanofiber network composite membrane was first introduced by the present authors in Ref. 24, where the steps for fabricating such a membrane were described. Those membranes contained 2.5 mmol/g IEC sPAES electrospun nanofibers with no sPOSS. After compaction, welding, and impregnation, the proton conductivity of the final membrane in water at room temperature was lower than that of commercial Nafion. To increase proton conductivity, nanofiber mats in the present study were electrospun from a mixture of 2.1 mmol/g IEC sPAES with sPOSS (where the sPAES/sPOSS weight ratio was 60/40). Attempts to electrospin sPAES/sPOSS nanofibers from a dimethylacetamide (DMAc) solution (as was done in Ref. 24) were unsuccessful due to the precipitation of sPOSS. The use of isopropanol or methanol solvents was also unsuccessful because these alcohols were too volatile (resulting in electrosprayed droplets as opposed to the desired electrospun fibers). The solubility and excessive volatility problems were resolved by using 2-butoxyethanol as the electrospinning solvent. A comparison of the conditions for electrospinning sPAES nanofibers from DMAc (2.5 mmol/g IEC with no sPOSS)

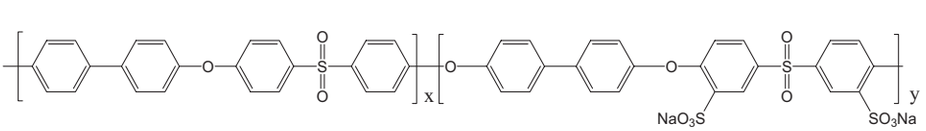

Figure 2. Chemical structure of sPAES. The values of *x* and *y* for 2.1 mmol/g IEC sPAES were 0.48 and 0.52, respectively.

Table I. Electrospinning conditions for sPAES and sPAES + sPOSS nanofiber mats.

	sPAES (2.5 mmol/g) [a]	sPAES (2.1 mmol/g)	sPAES (2.1 mmol/g) +40 wt % sPOSS
Solution composition	25 wt % sPAES 75 wt % DMAc	30 wt % sPAES 70 wt % 2-butoxyethanol	24 wt % sPAES 16 wt % sPOSS 60 wt % 2-butoxyethanol
Applied voltage (kV)	14	7	14
Spinneret-to-collector distance (cm)	8	6	6
Solution flow rate (mL/h)	0.04	0.05	0.05

[a] Results from Ref. 24.

and 2-butoxyethanol (2.1 mmol/g IEC with and without sPOSS) is presented in Table I. The three most important processing parameters for electrospinning were solution concentration, voltage between the spinneret needle and drum collector, and polymer solution flow rate. These parameters were systematically adjusted to obtain high quality continuous nanofibers with no droplets or beads.

The scanning electron micrographs (SEMs) of the structures obtained after each membrane fabrication step (nanofiber electrospinning, mat compaction, fiber welding, and mat impregnation) are presented in Fig. 3 for fibers composed of 2.1 mmol/g IEC sPAES (no sPOSS). The number-averaged fiber diameter in the initial mat was 292 nm (see Fig. 3a) with a fiber volume fraction of 0.20. The fiber diameter with 2-buthoxyethanol was about twice that found when electrospinning from DMAc.[24] After compaction, the fiber volume fraction increased to ~0.60 (a volume fraction of 0.60 is shown in Fig. 3b), with a corresponding (proportional) decrease in mat thickness. Exposing the compacted mat to 2-butoxyethanol vapor introduced welds at fiber intersection points, which resulted in a slight increase in both the average fiber diameter and the fiber volume fraction (380 and 0.75 nm, respectively, in Fig. 3c). Finally, the inert polymer (NOA 63) was embedded into the mat, resulting in a dense membrane with no residual pores (Fig. 3d), where the final membrane thickness was 70 μm.

The proton conductivity of the 2.1 mmol/g IEC sPAES nanofiber composite membrane scaled linearly with the nanofiber volume fraction, i.e., the conductivity of a water-equilibrated nanofiber composite membrane at room temperature with a fiber volume fraction of 0.70 was 0.07 S/cm, as compared to 0.10 S/cm for a homogeneous (dense) membrane. Unfortunately, the proton conductivity of the 2.1 mmol/g IEC sPAES nanofiber membrane when equilibrated with water vapor at an activity <1.0 was below expectations [i.e., below the 2008 U.S. Department of Energy (DOE) target of 0.07 S/cm at 30°C and 80% RH]. To boost conductivity, the sPAES fibers were doped with a high IEC (4.8 mmol/g) sPOSS.

Nanofiber mats were fabricated from 2.1 mmol/g IEC sPAES with 40 wt % sPOSS. The electrospinning conditions listed in Table I produced unbeaded, small diameter fibers. A representative SEM of the resultant mat is shown in Fig. 4b. The sPOSS-containing fibers have a slightly greater diameter (average fiber diameter = 491 nm, see Fig. 4d) than those spun from only sPAES (average fiber diameter = 292 nm, see Fig. 4c). Also, some precipitation of sPOSS occurred outside the fibers. At present, it is not known whether this is only a surface effect (related to the partial sPOSS extraction by water that condensed on the mat surface during electrospinning) or a bulk phenomenon resulting from the limited solubility of sPOSS in sPAES. The final membrane was fabricated by compacting the mat, creating interfiber welds, and then embedding the mat with NOA 63 (using the same conditions as an sPAES mat with no sPOSS). An SEM of the final nanofiber network composite membrane cross section (after complete processing) is shown in Fig. 5. Good compatibility of the fibrous network with the NOA 63 matrix is evident, although it is difficult to distinguish single nanofibers

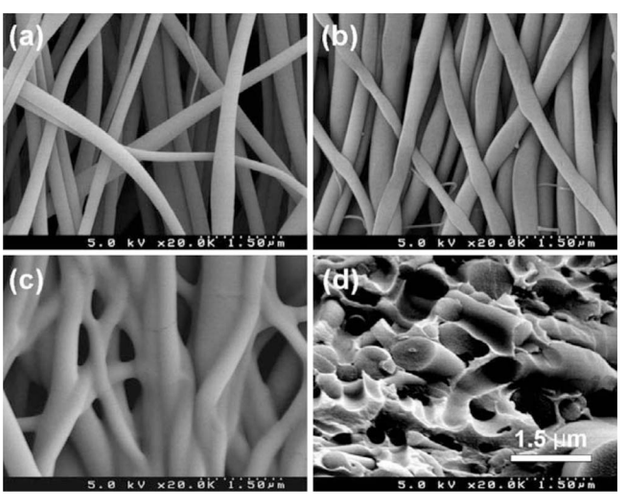

Figure 3. SEMs (20,000× magnification) of nanofiber structures obtained after successive membrane fabrication steps: (a) Surface of the as-spun mat, (b) surface of mat after compaction, (c) surface after mat compaction and fiber welding, and (d) cross section of the final membrane after embedding with NOA 63 polymer. The nanofibers were composed of 2.1 mmol/g IEC sPAES.

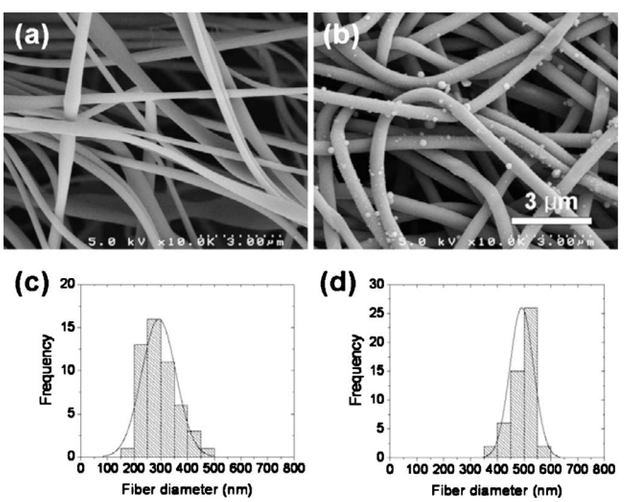

Figure 4. SEMs of (a) 2.1 mmol/g IEC sPAES, (b) 2.1 mmol/g IEC sPAES/sPOSS (60/40 w/w) nanofiber mats electrospun from 2-butoxyethanol at a magnification of 10,000×, (c) fiber diameter distribution histogram of 2.1 mmol/g sPAES nanofiber mat, and (d) fiber diameter distribution histogram of sPAES/sPOSS mat.

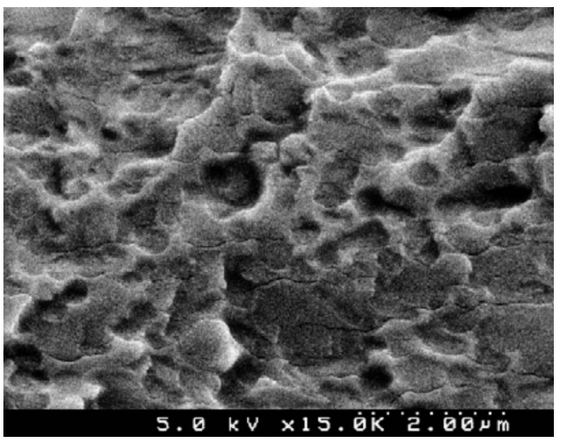

Figure 5. SEM of an embedded nanofiber network composite membrane cross section at a magnification of 15,000×. Nanofibers were composed of 2.1 mmol/g sPAES with 40 wt % sPOSS. The inert matrix polymer was NOA 63.

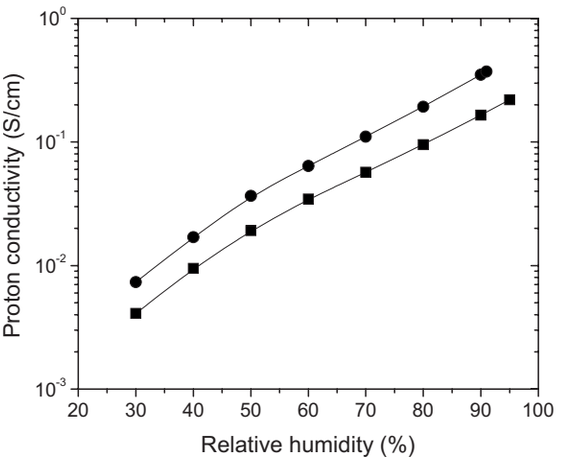

Figure 7. Proton conductivity dependence on RH for a nanofiber network composite membrane from sPAES (2.1 mmol/g IEC)/sPOSS (60/40 w/w) with a fiber volume fraction of 0.70. (■) 30 and (●) 80°C.

(only small, circular shadows indicate the presence of the welded fibrous network). The embedded nanofiber composite membranes had good mechanical strength and did not soften when exposed to high humidity air, contrary to what was observed for dense films cast from sPAES/sPOSS mixtures, which lost mechanical strength above an RH of 80%.

The proton conductivity of the composite membrane containing 40 wt % sPOSS in 2.1 mmol/g IEC sPAES nanofibers was measured at 30°C as a function of the RH. The results are shown in Fig. 6. Conductivity data for a nanofiber composite membrane without sPOSS and for a commercial Nafion 212 reference sample are also presented. The beneficial effect of adding sPOSS is clearly seen over the entire humidity range, where the proton conductivity of the sPAES/sPOSS nanofiber network composite membranes was significantly greater than that of a membrane with neat sPAES nanofibers. The beneficial effect of sPOSS was most evident at low humidity conditions, where the proton conductivity of aromatic polymers with sulfonic acid groups (such as sPAES) is particularly poor. The sPAES/sPOSS nanofiber network composite membrane was superior to Nafion in terms of proton conductivity at a humidity greater than

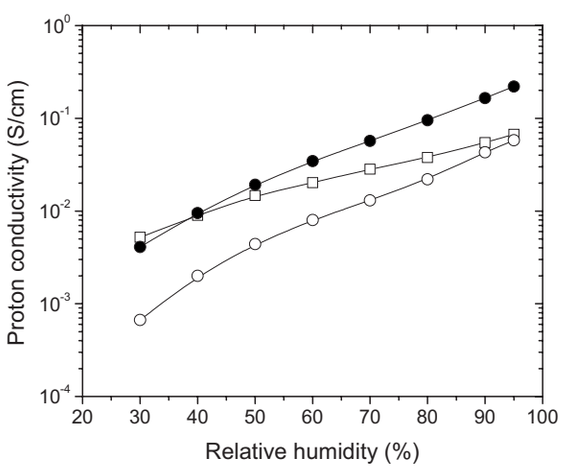

Figure 6. Proton conductivity as a function of RH at 30°C for nanofiber network composite membranes. (●) sPAES/sPOSS (60/40 w/w), (○) 2.1 mmol/g sPAES (without sPOSS), and (□) Nafion 212. The fiber volume fraction of the nanofiber network composite membranes was 0.70 and 0.75 for sPAES/sPOSS (60/40 w/w) and sPAES (no sPOSS), respectively.

40% RH. At 30°C and 80% RH (the DOE 2008 benchmark condition), the proton conductivity of a nanofiber network composite membrane with 40 wt% sPOSS and 2.1 mmol/g IEC sPAES fibers was 2.5 times greater than Nafion and 4.3 times greater than a neat sPAES nanofiber composite film.

The effect of temperature (30 and 80°C) on the proton conductivity of the nanofiber composite sPAES/sPOSS membrane for $30\% < RH < 95\%$ is shown in Fig. 7. The membrane conductivity increased 2-fold at $30\% < RH < 80\%$ when the temperature was raised from 30 to 80°C (no degradation of the membrane mechanical properties was observed at 80°C). The Arrhenius activation energy for proton conduction was 4.9 ± 0.5 kJ/mol and constant for membranes equilibrated in air with $20\% < RH < 80\%$. This proton conduction activation energy is significantly lower than that for Nafion 212 (measured as 7.8 kJ/mol at 90% RH and 13.8 kJ/mol at 20% RH). The lowered energy barrier for proton transport in the nanofiber network composite membrane is associated with the very high concentration of sulfonic acid groups of the percolating sPOSS particle network in the ionomer nanofibers. As a result, the sulfonate-to-sulfonate distance is much shorter than in a typical ionomer membrane like Nafion, and proton movement is less hindered energetically.

Proton conductivity is known to be a strong function of membrane water content, thus water retention is an important fuel cell membrane property, especially at low humidity. Equilibrium water-vapor sorption vs RH data at 30°C are shown in Fig. 8 for a neat sPAES nanofiber network composite membrane, the sPAES/sPOSS nanofiber network composite membrane 60/40 w/w sPAES/sPOSS, Nafion 212, and pure sPOSS (in powder form). Water-vapor uptake increased in all of the samples with increasing RH, where the differential increment (increase) in water sorption increased as RH increased (i.e., the change in water sorption with RH was highly nonlinear). Gravimetric water sorption of sPOSS was the highest and that of Nafion was the lowest among the samples tested. Water sorption of the sPAES nanofiber membrane (no sPOSS) was higher than that of Nafion 212 due to the very high IEC of sPAES, bordering on its water solubility limit.[25-27] Water sorption of the nanofiber composite containing sPOSS fell between the sPOSS and neat sPAES extremes but did not seem to follow closely a simple mixture rule.

Gravimetric water sorption was recalculated as the hydration number (λ, water molecules per sulfonic acid group) for sPAES nanofiber network membranes with 0 and 40 wt % sPOSS, where λ is calculated as

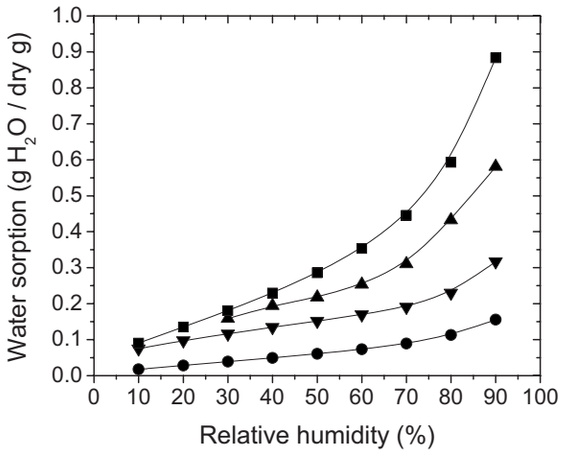

Figure 8. Equilibrium water-vapor sorption as a function of RH at 30°C (■) pure sPOSS, (▲) sPAES/sPOSS (60/40 w/w) nanofiber network membrane, (▼) 2.1 mmol/g IEC sPAES (no sPOSS) nanofiber network membrane, and (●) Nafion 212. Fiber volume fraction of the nanofiber network composite membranes was 0.70 and 0.75 for sPAES/sPOSS (60/40 w/w) and sPAES (no sPOSS), respectively.

$$\lambda = \frac{\text{gravimetric water sorption(g/g)}}{\text{MW}_{\text{H}_2\text{O}}\text{(g/mol)} \times \text{IEC}^{*}\text{(mmol/g)}} \times 1000\left(\frac{\text{mmol}}{\text{mol}}\right) \quad [1]$$

with the IEC of the polymer/particle fibers (IEC*) calculated as

$$\text{IEC}^{*} = (\text{weight fraction of sPAES} \times \text{IEC}_{\text{sPAES}}) + (\text{weight fraction of sPOSS} \times \text{IEC}_{\text{sPOSS}}) \quad [2]$$

The dependence of hydration number on RH at 30°C for sPAES and sPAES/sPOSS nanofiber composite membranes and for Nafion 212 is shown in Fig. 9. The sPAES/sPOSS composite film had the highest λ, especially at RH > 50%. The hydration number for the 60/40 w/w sPAES/sPOSS membrane at 90% RH was 14.5, which dropped to 2.5 when the RH was reduced to 10%. At low humidities (10–50% RH), the hydration numbers were the same for nanofiber composite membranes with and without sPOSS, but at high humidities, the sPAES/sPOSS films were clearly sorbing more waters per sulfonic acid group. Not surprisingly, the λ values for Nafion 212 were significantly lower than those with high IEC sPAES and sPAES/sPOSS.[27]

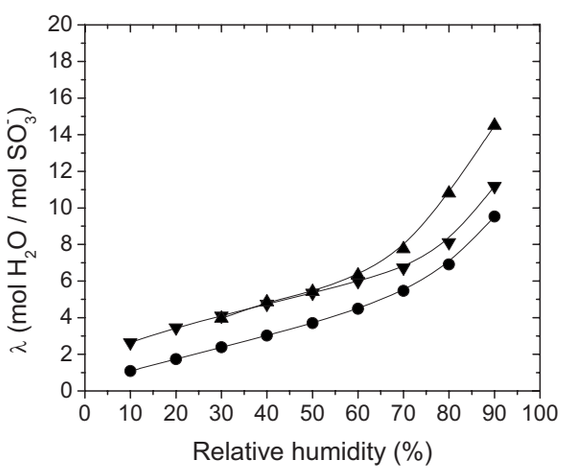

Figure 9. Hydration number (λ) as a function of RH at 30°C for nanofiber composite membranes. (▲) sPAES/sPOSS (60/40 w/w), (▼) 2.1 mmol/g IEC sPAES (no sPOSS), and (●) Nafion 212. Fiber volume fraction of the nanofiber network composite membranes was 0.70 and 0.75 for sPAES/sPOSS (60/40 w/w) and sPAES, respectively.

Based on the hydration number results, it is now possible to interpret the membrane conductivity vs RH data. At low humidity, the water retention of sPOSS is comparable to that of sPAES so hydration does not play an important role with respect to conductivity. Thus, it is the dramatic increase in the concentration of sulfonic acid groups upon addition of sPOSS to sPAES that boosts proton conduction; the total IEC of sPAES/sPOSS nanofibers (3.2 mmol/g) was more than 50% higher than that of neat sPAES (2.1 mmol/g). Due to the high acid strength of perfluorosulfonic acid moieties and the favorable hydrophilic/hydrophobic phase-separated cluster-type nanomorphology in Nafion, its proton conductivity is comparable to that of the higher IEC sPAES/sPOSS nanofiber membrane at humidities between 30 and 40%. At high humidities (RH > 50%), there is sufficient water in the sPAES/sPOSS nanofiber composite membrane for substantial dissociation of sulfonic acid groups and improved interconnectivity of water-filled channels, hence conductivity surpasses that of Nafion.

Conclusions

A class of sPAES–polyurethane (NOA63) nanofiber network composite membranes containing sPOSS was designed, and a series of films was fabricated and characterized in terms of proton conductivity and water uptake. The membranes were tested at 30°C and their proton conductivity and water uptake were superior to those measured for pristine sPAES nanofibers or a homogeneous (commercial) Nafion membrane. At 80% RH, a nanofiber composite membrane with an sPOSS loading of 40 wt % (based on the nanofiber weight) had proton conductivity exceeding that of Nafion by a factor of 2.5 and that of pristine nanofiber sPAES membranes by a factor of 4.3. Water uptake in the sPAES/sPOSS nanofiber network composite membranes was significantly greater than that of Nafion, e.g., 43 wt % for sPAES/sPOSS (60/40 w/w) membrane vs 11 wt % for Nafion 212 at 80% RH. The improvement in proton conductivity is associated with the very high IEC of the sPOSS nanoparticles. Normally, the addition of such highly charged material to a membrane results in excessive and undesirable swelling, which could be so great as to lower the effective concentration of protogenic groups (where the fixed-charge concentration is given as moles per unit volume of wet/swollen membrane), thereby lowering the proton conductivity. This did not occur in the nanofiber network composite membranes due to the presence of the inert matrix polymer, which effectively controlled membrane swelling.

Acknowledgment

The authors gratefully acknowledge the financial support of the U.S. Department of Energy, Energy Efficiency and Renewable Energy Program (grant DE-FG36-06GO16030).

Vanderbilt University assisted in meeting the publication costs of this article.

References

1. M. L. Einsla, Y. S. Kim, M. Hawley, H.-S. Lee, J. E. McGrath, B. Liu, M. D. Guiver, and B. S. Pivovar, *Chem. Mater.*, **20**, 5636 (2008).
2. X. Zhou, J. Weston, E. Chalkova, M. A. Hofmann, C. M. Ambler, H. R. Allcock, and S. N. Lvov, *Electrochim. Acta*, **48**, 2173 (2003).
3. Q. Guo, P. N. Pintauro, H. Tang, and S. O'Connor, *J. Membr. Sci.*, **154**, 175 (1999).
4. P. Dimitrova, K. A. Friedrich, B. Vogt, and U. Stimming, *J. Electroanal. Chem.*, **532**, 75 (2002).
5. F. Lufrano, V. Baglio, P. Staiti, A. S. Arico, and V. Antonucci, *Desalination*, **199**, 283 (2006).
6. A. K. Sahu, G. Selvarani, S. Pitchumani, P. Sridhar, and A. K. Shukla, *J. Electrochem. Soc.*, **154**, B123 (2007).
7. K. T. Adjemian, S. J. Lee, S. Srinivasan, J. Benziger, and A. B. Bocarsly, *J. Electrochem. Soc.*, **149**, A256 (2002).
8. M. L. Hill, Y. S. Kim, B. R. Einsla, and J. E. McGrath, *J. Membr. Sci.*, **283**, 102 (2006).
9. R. Jiang, H. R. Kunz, and J. M. Fenton, *Electrochim. Acta*, **51**, 5596 (2006).
10. A. K. Sahu, S. Pitchumani, P. Sridhar, and A. K. Shukla, *Fuel Cells*, **9**, 139 (2009).

11. Y. S. Kim, F. Wang, M. Hickner, T. A. Zawodzinski, and J. E. McGrath, *J. Membr. Sci.*, **212**, 263 (2003).
12. L. Li and Y. Wang, *J. Power Sources*, **162**, 541 (2006).
13. V. Ramani, H. R. Kunz, and J. M. Fenton, *Electrochim. Acta*, **50**, 1181 (2005).
14. M. Watanabe, H. Uchida, and M. Emori, *J. Phys. Chem. B*, **102**, 3129 (1998).
15. Y. S. Kim, L. Dong, M. A. Hickner, T. E. Glass, V. Webb, and J. E. McGrath, *Macromolecules*, **36**, 6281 (2003).
16. M. A. Hickner and B. S. Pivovar, *Fuel Cells*, **5**, 213 (2005).
17. J. Rozière and D. J. Jones, *Annu. Rev. Mater. Res.*, **33**, 503 (2003).
18. W. Apichatachutapan, R. B. Moore, and K. A. Mauritz, *J. Appl. Polym. Sci.*, **62**, 417 (1996).
19. P. L. Shao, K. A. Mauritz, and R. B. Moore, *Chem. Mater.*, **7**, 192 (1995).
20. M. Helen, B. Viswanathan, and S. S. Murthy, *J. Membr. Sci.*, **292**, 98 (2007).
21. L. Wang, B. L. Yi, H. M. Zhang, and D. M. Xing, *Electrochim. Acta*, **52**, 5479 (2007).
22. Y. Zhai, H. Zhang, J. Hu, and B. Yi, *J. Membr. Sci.*, **280**, 148 (2006).
23. M. H. Woo, O. Kwon, S. H. Choi, M. Z. Hong, H.-W. Ha, and K. Kim, *Electrochim. Acta*, **51**, 6051 (2006).
24. J. Choi, K. M. Lee, R. Wycisk, P. N. Pintauro, and P. T. Mather, *Macromolecules*, **41**, 4569 (2008).
25. K. D. Kreuer, *J. Membr. Sci.*, **185**, 29 (2001).
26. G. Alberti, M. Casciola, L. Massinelli, and B. Bauer, *J. Membr. Sci.*, **185**, 73 (2001).
27. W. L. Harrison, M. A. Hickner, Y. S. Kim, and J. E. McGrath, *Fuel Cells*, **5**, 201 (2005).